Research Article | Vol. 24, No. 15 | 25 Jul 2016 | OPTICS EXPRESS 17359

Optics EXPRESS

112 Gb/s transmission over 80 km SSMF using PDM-PAM4 and coherent detection without optical amplifier

XIAN ZHOU,[1,2] KANGPING ZHONG,[1,2,*] JIAHAO HUO,[1] LEI GAO,[4] YIGUANG WANG,[2] LIANG WANG,[2] YANFU YANG,[2] JINHUI YUAN,[2] KEPING LONG,[1] LI ZENG,[4] ALAN PAK TAO LAU,[3] AND CHAO LU[2]

[1]*Research Center for Convergence Networks and Ubiquitous Services, University of Science & Technology Beijing (USTB), No.30 Xue Yuan Road, Haidian, Beijing, China*
[2]*Photonics Research Centre, Department of Electronic and Information Engineering, The Hong Kong Polytechnic University, Hung Hom, Kowloon, Hong Kong, China*
[3]*Photonics Research Centre, Department of Electrical Engineering, The Hong Kong Polytechnic University, HungHom, Kowloon, Hong Kong, China*
[4]*Fixed Network Research and Development Department, Huawei Technologies Company, Sheng Zhen, China*
[*]*zhongkangping1987@gmail.com*

Abstract: Polarization-division-multiplexed (PDM) four-level pulse amplitude modulation (PAM4) with coherent detection is a promising low cost solution for 80 km inter-datacenter transmissions at 100 Gb/s and beyond. In this paper, three modified adaptive equalization algorithms for the PDM-PAM4 optical coherent systems, i.e. signal-phase aid least-mean-square (SP-LMS) algorithm, training multi-modulus algorithm (TMMA) and cascaded four-modulus algorithm (CMMA-4), are proposed and compared. Based on the proposed algorithms, 112 Gb/s PDM-PAM4 transmission over 80 km standard single mode fiber (SSMF) in C-band for a bit error rate (BER) below 3.8e-3 is successfully demonstrated without optical amplifier, chromatic dispersion (CD) pre-compensation and extra carrier recovery operations.

OCIS codes: (060.2330) Fiber optics communications; (060.4230) Multiplexing.

References and links

1. D. Ofelt, M. Nowell, and J. DAmbrosia, "400 Gigabit ethernet call-forinterest consensus," IEEE 802 Plenary Session, Orlando, FL USA, 2013.
2. K. Zhong, X. Zhou, T. Gui, L. Tao, Y. Gao, W. Chen, J. Man, L. Zeng, A. P. K. Lau, and C. Lu, "Experimental study of PAM-4, CAP-16, and DMT for 100 Gb/s Short Reach Optical Transmission Systems," Opt. Express **23**(2), 1176–1189 (2015).
3. J. Wei, Q. Cheng, R. Penty, I. White, and D. Cunningham, "400 Gigabit Ethernet using advanced modulation formats: Performance, complexity, and power dissipation," IEEE Commun. Mag. **53**(2), 182–189 (2015).
4. A. Dochhan, H. Griesser, N. Eiselt, M. H. Eiselt, and J. P. Elbers, "Solutions for 80km DWDM Systems," J. Lightwave Technol. **24**(2), 491–499 (2016).
5. L. Zhang, T. Zuo, Y. Mao, Q. Zhang, E. Zhou, G. N. Liu, and X. Xu, "Beyond 100-Gb/s Transmission Over 80-km SMF Using Direct-Detection SSB-DMT at C-Band," J. Lightwave Technol. **34**(2), 723–729 (2016).
6. D. Che, A. Li, X. Chen, Q. Hu, Y. Wang, and W. Shieh, "Stokes Vector Direct Detection for Linear Complex Optical Channels," J. Lightwave Technol. **33**(3), 678–684 (2015).
7. P. Dong, X. Chen, K. Kim, S. Chandrasekhar, Y. K. Chen, and J. H. Sinsky, "128-Gb/s 100-km transmission with direct detection using silicon photonic Stokes vector receiver and I/Q modulator," Opt. Express **34**(13), 14208–14214 (2016).
8. C. Xie, P. Dong, P. Winzer, C. Gréus, M. Ortsiefer, C. Neumeyr, S. Spiga, M. Müller, and M. C. Amann, "960-km SSMF transmission of 105.7-Gb/s PDM 3-PAM using directly modulated VCSELs and coherent detection," Opt. Express **21**(9), 11585–11589 (2013).
9. C. Xie, S. Spiga, P. Dong, P. Winzer, M. Bergmann, B. Kögel, C. Neumeyr, and M. Amann, "Generation and transmission of a 400-Gb/s PDM/WDM signal using a monolithic 2x4 VCSEL array and coherent detection," in Optical Fiber Communication Conference (OFC), San Francisco, California, 2014, paper Th5C.9.
10. S. Haykin, B. Widrow, *Least-Mean-Square Adaptive Filters*, (John Wiley & Sons 31, 2003).

#261931 http://dx.doi.org/10.1364/OE.24.017359
Journal © 2016 Received 28 Mar 2016; revised 27 Jun 2016; accepted 14 Jul 2016; published 22 Jul 2016

Optics EXPRESS

11. X. Zhou, L. E. Nelson, P. Magill, R. Isaac, B. Zhu, D. W. Peckham, P. I. Borel, and K. Carlson, "High spectral efficiency 400 Gb/s transmission using PDM time-domain hybrid 32–64 QAM and training-assisted carrier recovery," J. Lightwave Technol. **31**(7), 999–1005 (2013).
12. M. Kuschnerov, F. N. Hauske, K. Piyawanno, B. Spinnler, M. S. Alfiad, A. Napoli, and B. Lankl, "DSP for coherent single-carrier receivers," J. Lightwave Technol. **27**(16), 3614–3622 (2009).
13. D. N. Godard, "Self-Recovering Equalization and Carrier Tracking in Two-Dimensional Data Communication Systems," IEEE Trans. Commun. **28**(11), 1867–1875 (1980).
14. J. T. Yuan and T. C. Lin, "Equalization and carrier phase recovery of CMA and MMA in blind adaptive receivers," IEEE Trans. Signal Process. **58**(6), 3206–3217 (2010).
15. J. Yang, J. J. Werner, and G. A. Dumont, "The multimodulus blind equalization and its generalized algorithms," IEEE J. Sel. Areas Comm. **20**(5), 997–1015 (2002).
16. F. Machi, M. S. Alfiad, M. Kuschnerov, T. Wuth, D. van den Borne, N. Hanik, and H. de Waardt, "111-Gb/s PolMux-quadrature duobinary for robust and bandwidth efficient transmission," IEEE Photonics Technol. Lett. **22**(11), 751–753 (2010).
17. X. Zhou, J. Yu, and P. Magill, " Cascaded two-modulus algorithm for blind polarization de-multiplexing of 114-gb/s pdm-8qam optical signals. " in Optical Fiber Communication Conference (OFC), 2009, paper. OWG3.
18. X. Zhou and J. Yu, "Multi-level, multi-dimensional coding for high-speed and high-spectral- efficiency optical transmission," J. Lightwave Technol. **27**(16), 3641–3653 (2009).
19. J. Zhang, J. Yu, N. Chi, Z. Dong, J. Yu, X. Li, L. Tao, and Y. Shao, "Multi-Modulus Blind Equalizations for Coherent Quadrature Duobinary Spectrum Shaped PM-QPSK Digital Signal Processing," J. Lightwave Technol. **31**(7), 1073–1078 (2013).
20. P. J. Winzer, A. H. Gnauck, C. R. Doerr, M. Magarini, and L. L. Buhl, "Spectrally efficient long-haul optical networking using 112-Gb/s polarization-multiplexed 16-QAM," J. Lightwave Technol. **28**(4), 547–556 (2010).

1. Introduction

The ever-increasing broadband mobile communication, cloud computing services and video applications are driving the transmission rate growth of the datacenter interconnects. In the near future, 100 Gb/s or above per wavelength will be necessary for the short reach systems [1]. In order to satisfy the requirements of low cost and simple implementation for short reach applications, advanced modulation formats with intensity modulation and direct detection (IM-DD), including pulse amplitude modulation (PAM), carrier-less amplitude modulation (CAP) and discrete multi-tone (DMT), have been widely investigated and demonstrated [2,3]. According to currently discussed solutions for 80 km transmission inter-data center connections at 100G line rate, an optical pre-amplifier is necessary if IM-DD approaches are used [4]. Even with the use of optical amplifier, however, it is still difficult for IM-DD systems to achieve 100G transmission over 80km of SSMF using single wavelength. Therefore, it is necessary to find other single wavelength solutions for 80 km and 100 Gb/s transmission. In [5], L. Zhang *et. al.* employed a dual-driver Mach-Zehnder modulator (DD-MZM) to generate a SSB-DMT signal at the transmitter, and demonstrated a 105 Gb/s SSB-DMT transmission over 80 km SSMF in C-band using direct detection with erbium doped fiber amplifiers (EDFA). D. Che *et. al.* proposed a signal-carrier polarization multiplexing with Stokes vector direct detection (SV-DD) scheme [6]. Recently, they have also demonstrated 128 Gb/s SV-DD transmission over 100 km SSMF using silicon photonic Stokes vector receiver and I/Q modulator [7]. However, in all the proposed direct detection solutions, optical amplifier and Mach-Zehnder modulator (MZM) are necessary.

In contrast to direct-detection technique, digital coherent detection is a powerful approach to mitigate channel dispersion and increase receiver sensitivity. Besides, the cost of optical coherent systems can be effectively reduced by combining with intensity modulated transmitter. In [8,9], intensity-modulation-based coherent detection was first employed by C. Xie *et. al.* for metro network applications (toward 100~1000 km) with in-line and optical preamplifiers. To achieve single wavelength 100 Gb/s over 80 km transmission for inter-datacenter connections, four-level pulse amplitude modulation (PAM4) with polarization-division-multiplexing (PDM) and coherent detection is an attractive solution due to cost and size concerns. In such a system, electro-absorption modulated laser (EML) can be used as the transmitter. The size is less than a fifth of MZM, and its cost will be half of that of MZM. The sensitivity advantage brought about by coherent detection ensures that no in line and optical pre-amplifiers are necessary for the 80km transmission target. Our investigation, however,

Optics EXPRESS

show that typical adaptive equalization algorithms designed for high order modulation formats such as QPSK and QAM will not work well for PDM-PAM4. To solve this problem, here we propose three modified algorithms for coherent optical PDM-PAM4 systems, including signal-phase aid least-mean-square algorithm (SP-LMS), training multi-modulus algorithm (TMMA) and cascaded four-modulus algorithm (CMMA-4), and study their performance experimentally. With the proposed algorithms, we successfully demonstrate a 112 Gb/s PDM-PAM4 transmission over 80-km SSMF with a typical bit error rate (BER) threshold of hard-decision forward-error correction (FEC) codes (BER<3.8e-3), without any optical amplifier, CD pre-compensation and extra carrier recovery operations.

2. Problem with existing adaptive equalization algorithms

For high speed optical systems, it is necessary to use adaptive digital equalizer to compensate for linear distortions incurred by channel dispersion or system bandwidth limitation. Figure 1 illustrates four equalization modes (i.e. *Training Mode*, *Blind Mode*, *Radius-Directed* (*RD*) *Mode*, and *Decision-Directed* (*DD*) *Mode*) for error computation and update of equalizer taps, depending on different existing adaptive algorithms, as described below.

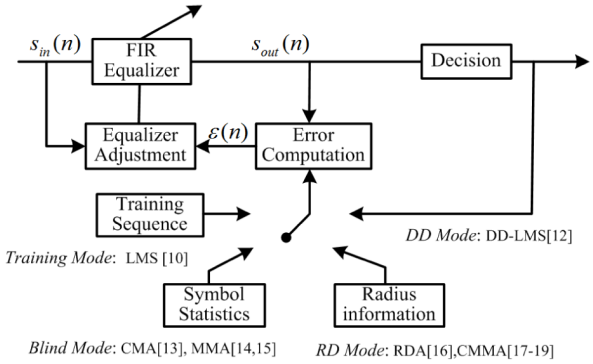

Fig. 1. Digital equalizer based on different adaptive equalization algorithms.

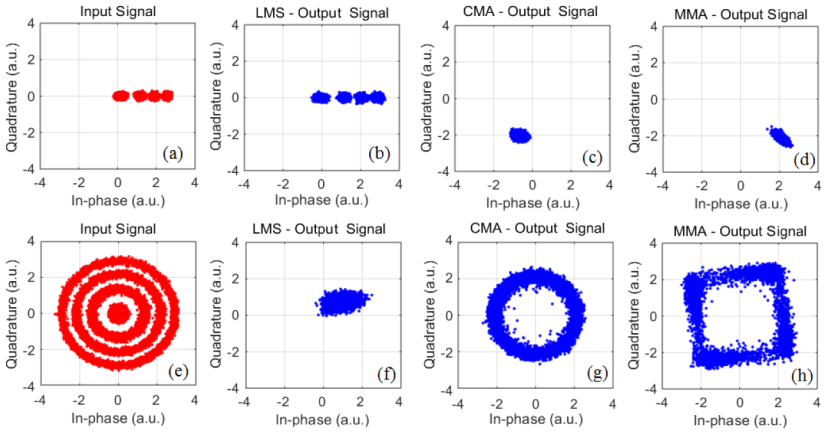

Fig. 2. (a) Input signal distributions for 28Gbaud PAM4 and (e) with the influence of carrier phase distortions. (b, f) after LMS-based equalization, (c, g) after CMA-based equalization, (d, h) after MMA-based equalization. (By simulation).

The least-mean-square algorithm (LMS) is a classic equalization algorithm [10], which can work in *Training Mode* and *DD Mode*. In order to distinguish its two modes of operation, LMS and DD-LMS are used respectively, as shown in Fig. 1. For LMS-based equalizer, the tap coefficients can be adaptively determined by minimizing the error between s_{out} and the

Optics EXPRESS

reference signal. However, LMS algorithm is very sensitive to carrier phase impairment. For example, as shown in Fig. 2(f), in the presence of carrier phase offset PAM4 signal will not converge to four levels as in Fig. 2(b). Therefore, standard LMS has to be preceded or combined with the carrier recovery in order for it to be used to equalize channel distortions, such as in [11,12]. However, PAM signal does not encode information on carrier frequency and phase. It will be costly to employ extra carrier frequency and phase estimations in the intensity modulation based system. In addition, large phase noise associated with low cost EML may prevent the algorithm to work properly.

In contrast to LMS, the constant modulus algorithm (CMA) [13] is most widely adopted algorithm in *Blind Mode* operation with the benefit that no information about the carrier phase is required. It updates the coefficients to minimize the variance between the samples and a constant modulus. However, CMA is only suitable for signals with arbitrary symmetric two-dimensional signal constellation [13,14], such as QPSK and M-PSK. It can also work well even when the modulus is not constant, such as when higher order QAM is used. However, as shown in Fig. 2(c) and 2(g)), it will not work well for PAM4. Mutimodulus algorithm (MMA) [14,15] is another blind algorithm with some ability of carrier phase recovery. Its cost functions are calculated for the real and imaginary components independently, to force the output symbol round separate straight contours. However, it will breakdown once the phase impairment is over its tolerance. Therefore, MMA cannot be used for PDM-PAM4 signal in the presence of carrier frequency offset and large laser phase noise (~MHz) either. Furthermore, it has the same characteristics as CMA, it is only suitable for signals with symmetric constellation, but is not suitable to the PDM-PAM4 system, as demonstrated in Fig. 2(d) and 2(h).

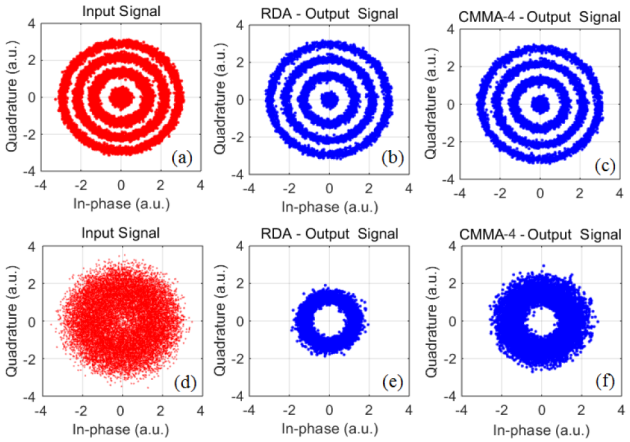

Fig. 3. (a) Input signal constellations for 28 Gbaud PAM4 in the presence of carrier phase distortions and (d) with 200 ps/nm of CD. (b, e) after RDA-based equalization; (c, f) after CMMA-4 - based equalization. (By simulation).

In order to solve the non-optimal convergence problem of CMA for modulation formats that do not have constant amplitude such as QAM, some radius-related algorithms have been proposed, such as the radius-directed algorithm (RDA) [16] and the cascaded multi-modulus algorithm (CMMA) for 8QAM [17], 16QAM [18] and quadrature duobinary (DQB) QPSK [19]. However, correct decisions of signal radiuses are required for RDA and CMMA. It is difficult to handle the received signal with serious channel distortions by using RDA and CMMA directly. In practice, CMA algorithm is used to achieve initial convergence. When the "eye is open", CMA-based equalizer is then switched to RDA or CMMA algorithms [20]. To compare Fig. 3(b) with Fig. 3(e), and Fig. 3(c) with Fig. 3(f), it can be seen that RDA and CMMA have the similar properties when used for PAM4 signal, with even lower tolerance to channel dispersion. It should be mentioned that since there is no available CMMA algorithms

Optics EXPRESS

for PAM4 signal, the results of Fig. 3(c) and 3(f) are obtained by using our modified CMMA-4. (Please see Section. 3.3 for details.) In view of above mentioned problems, therefore, it is necessary to propose an equalization algorithm for PDM-PAM4, making the PAM4-based equalizer robust against channel dispersion, carrier frequency offset and laser linewidth, without the need for carrier recovery.

3. Modified algorithms for PDM-PAM4 signal

3.1 Signal-phase aided least-mean-square algorithm (SP-LMS)

As mentioned before, PAM signal does not encode information on carrier frequency and phase, it will be costly to employ extra carrier frequency and phase estimations providing phase information to the LMS. In this case, we propose a modified LMS-based algorithm, i.e. SP-LMS, which can avoid the phase-induced influence simply and efficiently. In SP-LMS, the phase of the equalized signal is extracted directly and added to the reference signal to calculate the error function, as illustrated in Fig. 4.

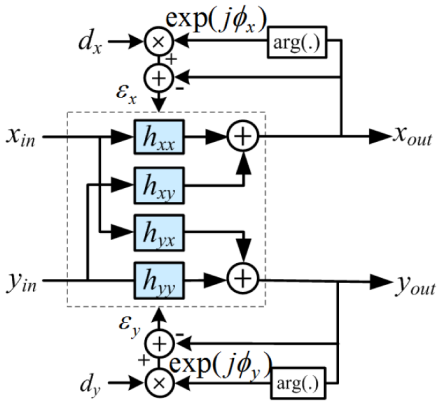

Fig. 4. Block diagram of the SP-LMS-based equalization.

The SP-LMS error functions of the two polarizations at the n^{th} iteration are given by

$$\varepsilon_x^{(n)} = \exp\left(j\phi_x^{(n)}\right) d_x^{(n)} - x_{out}^{(n)},\ \varepsilon_y^{(n)} = \exp\left(j\phi_y^{(n)}\right) d_y^{(n)} - y_{out}^{(n)} \tag{1}$$

where $d_{x(y)}$ denotes the PAM4-based reference signal and $\phi_{x(y)}$ is the phase of the output signal after equalization, which can be easily extracted by,

$$\phi_x^{(n)} = \arg\left(x_{out}^{(n)}\right),\quad \phi_y^{(n)} = \arg\left(y_{out}^{(n)}\right) \tag{2}$$

Based on the stochastic gradient algorithm, the tap coefficients of SP-LMS can be updated according to,

$$\begin{aligned} \mathbf{h}_{xx}^{(n+1)} &= \mathbf{h}_{xx}^{(n)} + \mu \cdot \varepsilon_x^{(n)} \cdot \mathbf{x}_{in}^{*(n)},\ \mathbf{h}_{xy}^{(n+1)} = \mathbf{h}_{xy}^{(n)} + \mu \cdot \varepsilon_x^{(n)} \cdot \mathbf{y}_{in}^{*(n)} \\ \mathbf{h}_{yx}^{(n+1)} &= \mathbf{h}_{yx}^{(n)} + \mu \cdot \varepsilon_y^{(n)} \cdot \mathbf{x}_{in}^{*(n)},\ \mathbf{h}_{yy}^{(n+1)} = \mathbf{h}_{yy}^{(n)} + \mu \cdot \varepsilon_y^{(n)} \cdot \mathbf{y}_{in}^{*(n)} \end{aligned} \tag{3}$$

where $\mathbf{h}_{xx}$, $\mathbf{h}_{xy}$, $\mathbf{h}_{yx}$, and $\mathbf{h}_{yy}$ are the vectors of the butterfly filter tap weights, $\mathbf{x}_{in}$ and $\mathbf{y}_{in}$ are the equalizer input data vector in X-pol and Y-pol respectively, μ is the convergence parameter, and ()* denotes complex conjugate.

The same as the standard LMS algorithm, SP-LMS has two operation modes, i.e. *Training Mode* and *DD Mode*. In the *Training Mode*, the reference signal $d_{x(y)}$ is provided by training

Optics EXPRESS

sequence. After convergence, SP-LMS-based equalizer can be switched to *DD Mode*. In this case, $d_{x(y)}$ is the decision feedback value of the equalized PAM4 signal, as

$$d_x^{(n)} = \text{Decision}\left(\left|x_{out}^{(n)}\right|\right),\quad d_y^{(n)} = \text{Decision}\left(\left|y_{out}^{(n)}\right|\right) \tag{4}$$

3.2 Training multi-modulus algorithm (TMMA)

TMMA is a modified CMA algorithm, which is only implemented on the signal amplitude. Hence, it is robust against the carrier frequency offset and laser linewidth inherently. However, the blind equalization characteristic of CMA cannot be preserved for TMMA. Its convergence must to depend on training sequence. Figure 5 shows the block diagram of adaptive equalizer based on TMMA algorithm.

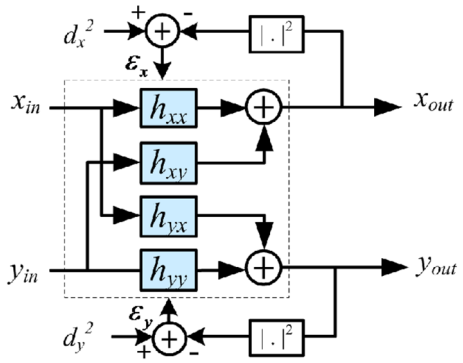

Fig. 5. Block diagram of the TMMA-based equalization.

The TMMA error functions of two polarizations at the n^{th} iteration are given by,

$$\varepsilon_x^{(n)} = \left(d_x^{(n)}\right)^2 - \left|x_{out}^{(n)}\right|^2, \varepsilon_y^{(n)} = \left(d_y^{(n)}\right)^2 - \left|y_{out}^{(n)}\right|^2 \tag{5}$$

where $|.|^2$ stands for returning the power of the input signal, and $d_{x(y)}$ also denotes the reference signal that is provided by training sequence before equalization converged. Then the tap weights of TMMA are updated as same as the basic CMA, based on the following equations:

$$\begin{aligned} \mathbf{h}_{xx}^{(n+1)} &= \mathbf{h}_{xx}^{(n)} + \mu \cdot \varepsilon_x^{(n)} \cdot x_{out}^{(n)} \cdot \mathbf{x}_{in}^{*(n)},\ \mathbf{h}_{xy}^{(n+1)} = \mathbf{h}_{xy}^{(n)} + \mu \cdot \varepsilon_x^{(n)} \cdot x_{out}^{(n)} \cdot \mathbf{y}_{in}^{*(n)} \\ \mathbf{h}_{yx}^{(n+1)} &= \mathbf{h}_{yx}^{(n)} + \mu \cdot \varepsilon_y^{(n)} \cdot y_{out}^{(n)} \cdot \mathbf{x}_{in}^{*(n)},\ \mathbf{h}_{yy}^{(n+1)} = \mathbf{h}_{yy}^{(n)} + \mu \cdot \varepsilon_y^{(n)} \cdot y_{out}^{(n)} \cdot \mathbf{y}_{in}^{*(n)} \end{aligned} \tag{6}$$

Comparing to CMA, the training-based cost function $E(d_{x,y}{}^2\text{-}|x(y)_{out}|^2)^2$ of TMMA can avoid the local minimum problem effectively for achieving a correct and stable convergence. After the equalizer converged, the same as SP-LMS, the TMMA-based equalizer will be switched to *DD Mode*. We should mention that the TMMA algorithm in *DD Mode* can be seen as RDA algorithm [16], since to determine the nearest radius for the equalizer output is the equivalent of decision process in the PDM-PMA4 system.

3.3 *Cascaded four-modulus algorithm* (CMMA-4)

The CMMA algorithm is another *Radius Mode* algorithm. In view of that current CMMA algorithms proposed for 8QAM [17], 16QAM [18] or DQB-QPSK [19], are not suitable for PAM4 signal, we have also modified CMMA algorithm for PDM-PAM4 signal. For the CMMA algorithm, multiple reference circles are introduced in a cascaded way such that the final error approaches zero for an ideal signal.

Optics EXPRESS

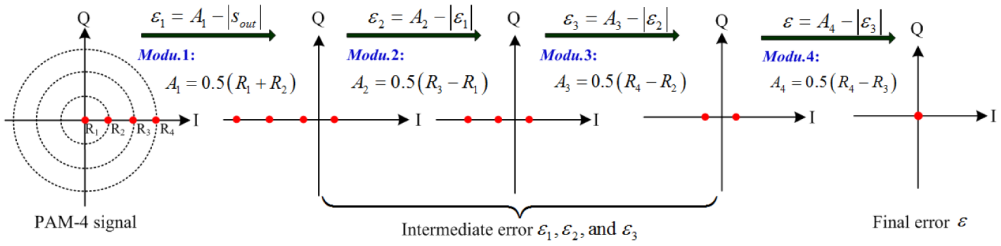

Fig. 6. Illustration of CMMA-4 for PAM4 signal.

Figure 6 illustrates how to calculate the error signal using the modified CMMA-4 algorithm for the PAM4 signal. Here, four reference moduli $A_1 = 0.5(R_1 + R_2)$, $A_2 = 0.5(R_3 - R_1)$, $A_3 = 0.5(R_4 - R_2)$, and $A_4 = 0.5(R_4 - R_3)$ are defined to make the final error of PAM4 approach zero.The CMMA-4 error functions of two polarizations at the n^{th} iteration are given by,

$$\begin{aligned} \varepsilon_x^{(n)} &= A_4 - \left| A_3 - \left| A_2 - \left| A_1 - \left| x_{out}^{(n)} \right| \right| \right| \right| \\ \varepsilon_y^{(n)} &= A_4 - \left| A_3 - \left| A_2 - \left| A_1 - \left| y_{out}^{(n)} \right| \right| \right| \right| \end{aligned} \tag{7}$$

where |. | stands for returning the absolute value of the input. In the CMMA-based equalization, the additional sign calculations of errors are required as

$$\begin{aligned} e_{x,y}^{(n)} = -\text{sign}\left(x, y_{out}^{(n)}\right) \cdot \text{sign}\left(A_1 - \left|x, y_{out}^{(n)}\right|\right) \cdot \text{sign}\left(A_2 - \left|A_1 - \left|x, y_{out}^{(n)}\right|\right|\right) \\ \cdot \text{sign}\left(A_3 - \left|A_2 - \left|A_1 - \left|x, y_{out}^{(n)}\right|\right|\right|\right) \end{aligned} \tag{8}$$

where sign (.) is a signum function. As the other CMMA algorithms, the modified CMMA-4 algorithm has the same updating equations, which are given by

$$\begin{aligned} \mathbf{h}_{xx}^{(n+1)} &= \mathbf{h}_{xx}^{(n)} + \mu \cdot \varepsilon_x^{(n)} \cdot e_x^{(n)} \cdot \mathbf{x}_{in}^{*(n)}, \quad \mathbf{h}_{xy}^{(n+1)} = \mathbf{h}_{xy}^{(n)} + \mu \cdot \varepsilon_x^{(n)} \cdot e_x^{(n)} \cdot \mathbf{y}_{in}^{*(n)} \\ \mathbf{h}_{yx}^{(n+1)} &= \mathbf{h}_{yx}^{(n)} + \mu \cdot \varepsilon_y^{(n)} \cdot e_y^{(n)} \cdot \mathbf{x}_{in}^{*(n)}, \quad \mathbf{h}_{yy}^{(n+1)} = \mathbf{h}_{yy}^{(n)} + \mu \cdot \varepsilon_y^{(n)} \cdot e_y^{(n)} \cdot \mathbf{y}_{in}^{*(n)} \end{aligned} \tag{9}$$

As shown in Fig. 3(f), CMMA-4 cannot be used in the initial filter convergence stage. Based on the robust training-based equalization, such as SP-LMS or TMMA, the CMMA-4 can be switched instead of using *DD Mode*. Table1. classifies the modified PDM-PAM4 equalization algorithms for the different convergence stages.

Table 1. Proposed PDM-PAM4 Algorithms Classified for the Different Convergence Stages

For 1st conv. stage	For 2nd conv. stage
SP-LMS TMMA	SP-LMS with DD TMMA with DD (RDA) CMMA-4

4. Experimental setup and results

In the section, the performances of the modified algorithms, i.e. SP-LMS, TMMA and CMMA-4, are experimentally investigated in a 112 Gb/s PDM-PAM4 system, as shown in Fig. 7(a). At the transmitter, a DAC with a sampling rate of 56-GSam/s and 3dB bandwidth of 12GHz is used to generate the 28 Gbaud PAM4 driving signal (2 Samples/Symbol). The electric driving signal is boosted to a 1.7V peak-to-peak by a RF linear amplifier. Commercial electric absorption modulated laser (EML) with 3dB bandwidths of 30GHz was used to

Optics EXPRESS

modulate the PAM4 signal on to the optical carrier. The bias voltage is optimized to be −1.2 V. The center wavelength of the EML is 1546.1 nm. Here, the output power of the modulated signal is around 1 dBm. Then the single polarization PAM4 signal is fed into a polarization multiplexer, which is split and recombined in orthogonal polarizations after delaying one of the split signals to de-correlate it from another split signal. Then, the signal is launched into transmission link with 80km of SSMF. At the front-end of the receiver, a variable optical attenuator (VOA) is placed after SSMF to adjust the received optical power. Then, the received optical signal is detected by a commercial integrated coherent receiver (ICR) with 3dB bandwidths of 18GHz. Here, the power of the local oscillator is 13 dBm. Next, the detected signals are sampled by a real-time scope with a sampling rate of 80 GSa/s and 33 GHz bandwidth.

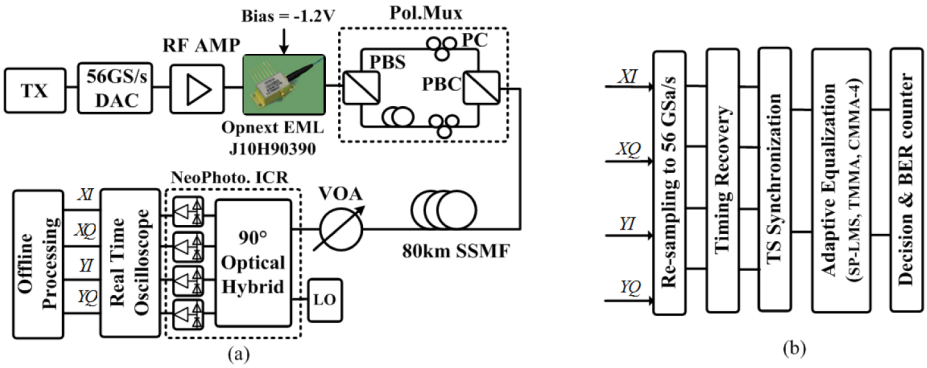

Fig. 7. (a) Experimental setup for 112Gbit/s PDM-PAM4 system, (b) offline DSP. DAC: digital-to-analog converter; PC: polarization controller; PBS: polarization beam splitter; PBC: polarization beam combiner; TS: training sequence.

Figure 7(b) shows offline signal processing procedure. The digital samples are re-sampled to two samples per symbol. After timing recovery by using digital squaring and filter algorithm, the correlation between the received samples and the training symbols is calculated to find the starting point of the training sequence from the coming data. This process is called TS synchronization, and note that the correlation calculation needs to be implemented on the power of the received samples so as to avoid the influence induced by carrier frequency offset and laser linewidth. Next, the butterfly-structured adaptive equalizer is employed to de-multiplex polarization, and compensate inter-symbol interferences induced by CD, PMD and the narrowband filtering effect. Here, the equalizer taps can be optimized by choosing the proposed algorithms, i.e. SP-LMS, TMMA and CMMA-4. Finally, the BER is measured by a bit error counter after symbol decision.

Optics EXPRESS

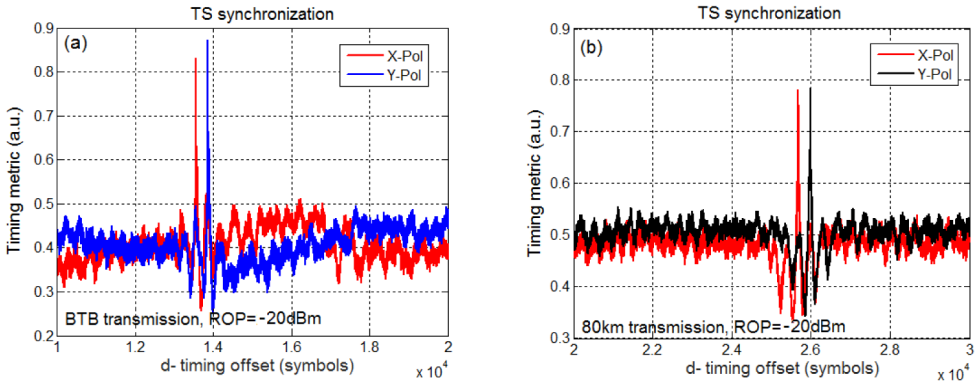

Fig. 8. Timing metric of TS synchronization for (a) BTB transmission at ROP = –20dBm, and (b) 80km SSMF transmission at ROP = –20dBm.

First, the performance of TS synchronization is investigated. Figure 8 shows the normalized timing metrics of back-to-back (BTB) and after 80 km SSMF transmission at a received optical power (ROP) of –20 dBm. Here, 1000 training symbols are used to calculate the correlation with the received signal. It can be seen that the location of the training symbols can be identified by finding the correlation peak. There is a location difference between X-pol and Y-pol (about 304 symbols), which reflects the delay operation implemented during polarization multiplexing at the transmitter. Comparing to Fig. 8(a) and 8(b), it can be seen that fiber dispersion will affect the magnitude of the correlation peak. Hence, a sufficient number of training symbols should be used for TS synchronization so as to avoid the correlation peak being submerged. In this paper, 1000 training symbols are used for TS synchronization in all the scenarios, and these training symbols are still used for the following adaptive equalization.

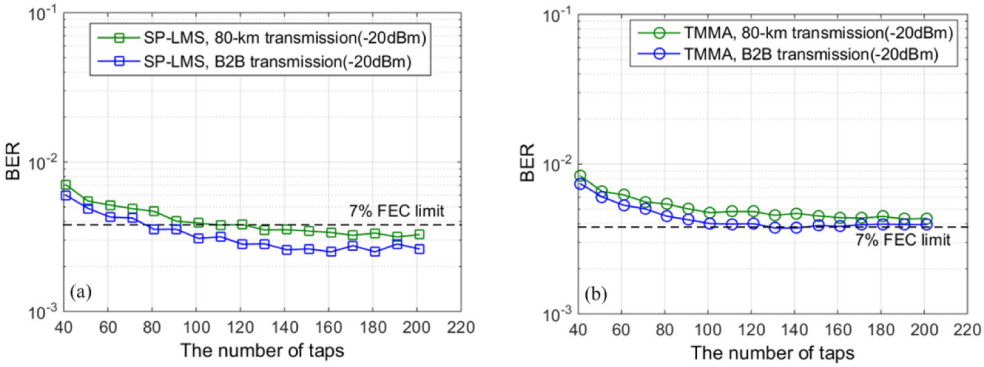

Fig. 9. BER as a function of the number of taps (a) by using SP-LMS algorithm, and (b) by using TMMA algorithm (ROP = –20dBm).

After locating the training symbols, the receiver samples will be equalized for de-multiplexing polarization and compensating for the transmission distortions. In order to obtain the best equalization performance, the effects of algorithm parameters are investigated in the 112 Gb/s PDM-PAM4 system. We first concern the proposed algorithms that can be applied to the first convergence stage, i.e. SP-LMS and TMMA algorithm. Figure 9(a) and 9(b) give BER performances as a function of the number of taps using the two algorithms respectively. Here, two transmission scenarios of BTB and 80 km SSMF transmissions are considered at a ROP of –20 dBm. Besides, the *Training Mode* is used here for the whole equalization process. It can be seen that stable BER performance can be achieved when the number of taps

Optics EXPRESS

is larger than 101 for both SP-LMS and TMMA algorithms. Furthermore, there is a similar trend of BER change with the number of taps for both BTB and 80 km fiber transmission, which indicates that the narrowband filtering effect introduced by the devices of transmitter and receiver, such as DAC and ICR, is more dominant impairment than CD distortion. In this case, the number of taps cannot be reduced by using CD compensator. Therefore, the extra CD compensation is not used before the adaptive equalizer in our system. All the kinds of ISI are compensated by using the adaptive butterfly equalizer.

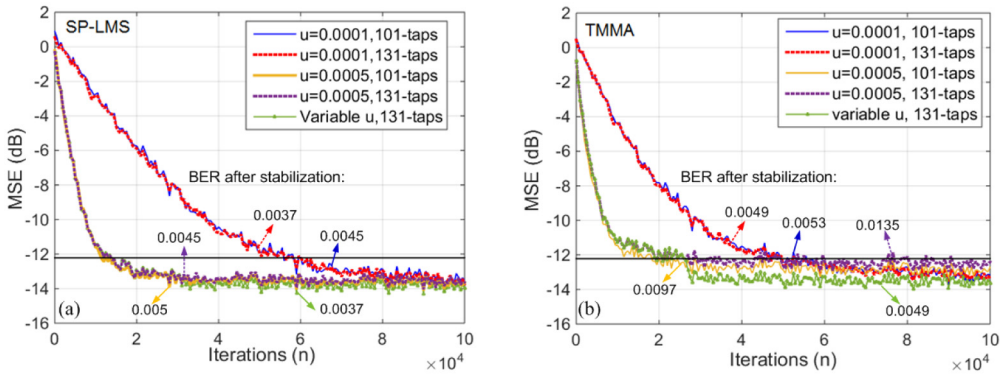

Fig. 10. Convergence properties with different step parameter - μ using (a) SP-LMS and (b) TMMA. MSE: mean square error. (After 80km transmission, ROP = −20dBm).

Then, the convergence properties of the SP-LMS and the TMMA algorithms are investigated respectively using different convergence parameters at a ROP of −20 dBm after 80km transmission (see Fig. 10(a) and 10(b)). It can be seen that the speed of convergence depends on the magnitude of μ, where a larger value results in faster convergence but also increases the residual error, and the SP-LMS algorithm has a smaller mean square error (MSE) on steady state than that of the TMMA. Since the tracking performance of equalizer is affected by the number of taps, we investigate the impact of different the number of taps on the convergence. However, it is hard to observe their difference on the convergence of MSE Therefore, BERs after equalizer stabilization for different parameter settings are also measured and shown in Fig. 10. The best BER of SP-LMS and TMMA are both obtained here with μ = 0.0005 and taps = 131. In order to achieve fast speed and high accuracy of convergence, we investigate the performance of SP-LMS and TMMA using a variable convergence parameter μ. In this case, μ is set to be 0.0005 at the beginning, and changed to 0.0001 after MSE smaller than −12 dB. As shown in Fig. 10, SP-LMS and TMMA can both reach their best BER result with rapid convergence speed using the variable μ.

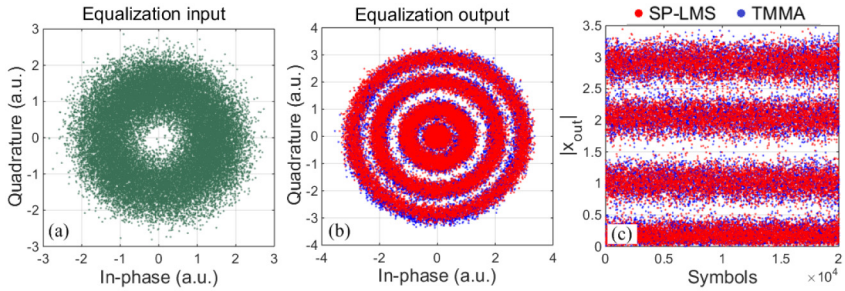

Fig. 11. Constellations of X-pol for (a) the input of equalizer, (b) the output of equalizer, and the absolute amplitude of the output of equalizer. (After 80km transmission, ROP = −20dBm).

Optics EXPRESS

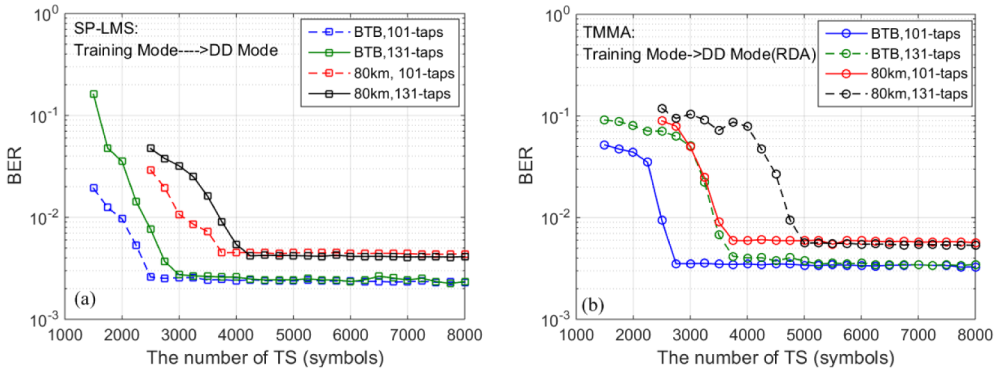

Fig. 12. BER as a function of the number of training symbols using (a) SP-LMS and (b) TMMA. (ROP = –20dBm).

Figure 11(a) and 12(b) show the constellation diagrams of the input and the output of equalizer after 80 km SSMF transmission at a ROP of –20 dBm. The output constellation with four-level circles demonstrates that ISI impairments can be successfully compensated by using the proposed SP-LMS and TMMA in the presence of phase distortion. As shown in Fig. 11(c), the decision operation can be implemented on the modulus value of the equalization output. In practice, the equalization process cannot always operate in the *Training Mode*. After the equalizer converges properly, the proposed SP-LMS and TMMA algorithms can be switched from *Training Mode* to *DD Mode*. In order to investigate how many training symbols are required to reach the switching condition, BER performances are measured as a function of the number of training symbols. In this case, at the end of the training symbols, the reference signal of SP-LMS and TMMA will be replaced by the decision values as shown in Eq. (4). It can be seen by comparing Fig. 12(a) with Fig. 12(b), the SP-LMS algorithm shows a faster speed to achieve the switching condition than that of TMMA. Besides, CD is a significant factor here. For 80 km fiber link about 1300 more training symbols are required than the case of BTB for both SP-LMS and TMMA. Moreover, the tap count is another factor affecting the number of training symbols required. As shown in Fig. 12(a) and 12(b), the larger the number of taps the larger the number of training symbols required for switching, this is especially true for TMMA algorithm. However, the BER performance is almost the same as long as the number of training symbols is sufficient for the equalizer to stabilize, which will not improve by increasing the number of training symbols.

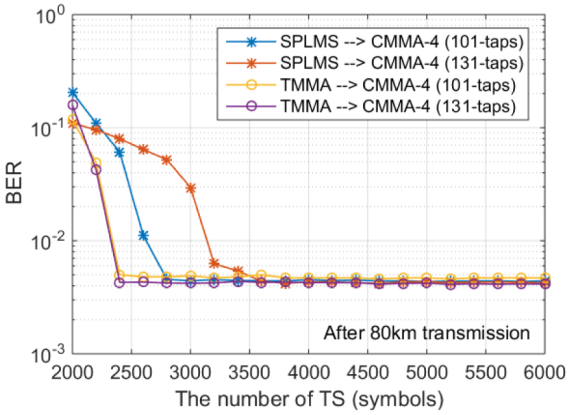

Fig. 13. BER as a function of the number of training symbols using (a) SP-LMS and (b) TMMA. (ROP = –20dBm).

Optics EXPRESS

In addition to SP-LMS and TMMA operated in the *DD Mode*, CMMA-4 is another switching option after the initial convergence. The BER performance is also investigated as a function of the amount of TS by using CMMA-4 in the second convergence stage. Comparing to Fig. 12, the less number of TS can be required by switching to the proposed CMMA-4 algorithm. It demonstrates that CMMA-4 has better tolerance against the residual distortion than that of SP-LMS and TMMA operated in the *DD Mode.* Besides, in contrast to combining with SP-LMS, CMMA-4 shows a better match with TMMA. The improvement is obvious for the combination of TMMA and CMMA, which can achieve a better BER performance and require much less the number of TS simultaneously than TMMA combined with itself in *DD Mode* operation.

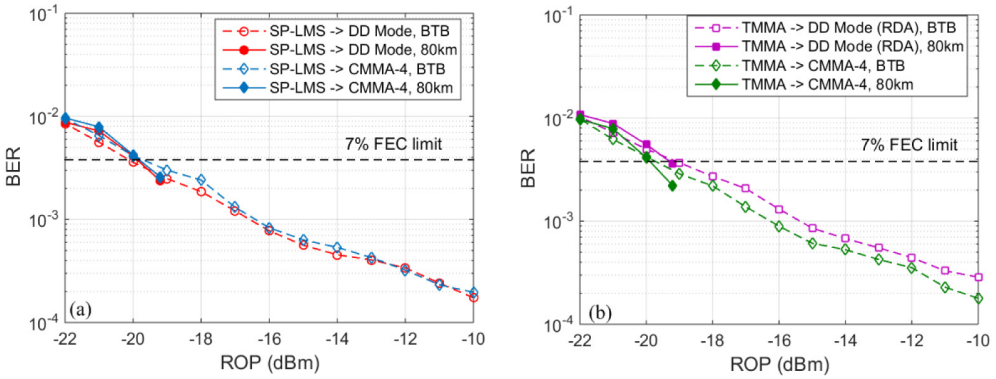

Fig. 14. BER as a function of ROP by using two different equalization algorithms.

Depending on different algorithm combinations, BER performances are measured as a function of ROP for BTB transmission and 80 km SSMF transmission. In order to give a fair compensation, the same number of taps (131 taps) is chosen for all the equalization algorithms, and in order to guarantee equalizer convergence at different ROPs, 6000 training symbols are used at the first stage of equalization (see Fig. 13). Since the equalizer will keep tracking and compensating channel distortion in *DD Mode* or *RD Mode* after initial convergence, TS is no longer required as long as channel has no drastic change. The overhead of TS can be neglected. In our experimental study, TS is only added in the initialization phase. Besides, because of no optical amplifier employed in the experimental system, the maximum ROP achieved is only about −19.2 dBm after 80 km transmission. It can be seen from Fig. 14, there is a negligible difference in ROP requirement between BTB and transmission scenarios. Comparing to TMMA combined with itself in the *DD Mode* operation, other three combination schemes have a similar performance, in which the BER reaches the hard-decision FEC threshold of 3.8e-3 at ROP of −20 dBm. In turn, a ROP sensitivity of −19.2 dBm is achieved for TMMA combined with itself in the *DD Mode* operation at the same BER threshold. The results show that 100 Gb/s short reach transmission over 80 km without optical amplifier can be achieved successfully using coherent optical PDM-PAM4.

5. Conclusion

In this paper, we propose three modified adaptive equalization algorithms, i.e. SP-LMS, TMMA and CMMA-4, for coherent optical PDM-PAM4 systems. The training-based SP-LMS and TMMA algorithms are robust against channel distortion in the presence of phase impairments, which can be employed at the beginning of equalization. After the initial convergence, three switching options are provided to keep tracking and compensating channel distortion, where SP-LMS with DD and CMMA-4 exhibited a better performance with respect to TMMA in the *DD Mode* operation. But no matter which algorithm is used, there are negligible differences in ROP requirements between BTB and transmission scenarios. Based

Optics EXPRESS

on the proposed algorithms, we have successfully demonstrated a 112 Gb/s transmission over 80 km SSMF in C-band for a bit error rate (BER) below 3.8e-3 by using PDM-PAM4 and coherent detection without optical amplifier, CD pre-compensation and extra carrier recovery operations.

Funding

The authors acknowledge the support of National Natural Science Foundation of China (NSFC) (61401020 and 61435006), Beijing Natural Science and Foundation (4154080), Hong Kong Government General Research Fund (GRF) PolyU 152079/14E, Hong Kong Scholars Program (XJ2013026), Fundamental Research Funds for the Central Universities (FRF-TP-15-028A2) and the Foundation of Beijing Engineering and Technology Center for Convergence Networks and Ubiquitous Services.